Indian Journal of Chemical Technology
Vol. 31, September 2024, pp. 673-680
DOI: 10.56042/ijct.v31i5.11274

Investigation of spectroscopic, water barrier and thermal characteristics of ameliorated chitosan membrane

Shivam Kumar[1], Devyanshu Sachdev[2], Renu Sharma[1] & Navneet Kaur Bhullar[2]*

[1]Department of Chemistry, University Institute of Science, Chandigarh University, Mohali, Punjab, India

[2]Department of Chemical Engineering, University Institute of Engineering, Chandigarh University, Mohali, Punjab, India

*E-mail: navneet.chemical@cumail.in / navneetbhullar@gmail.com

Received 20 May 2024; accepted 19 August 2024

The present research focuses on the ameliorated chitosan membrane (ACM) in which chitosan based membrane has been developed by optimization of different synthesis parameters such as the amount of solvent, amount of monomer and amount of initiator in which maximum percentage grafting of 812% is achieved. The synthesized membrane is further investigated for the evaluation of spectroscopic, water barrier and thermal characteristics. The spectroscopic studies are carried out using FTIR spectroscopy and UV-visible-NIR absorption spectroscopy which is used for evaluating the chemical characteristics. Water barrier characteristics are evaluated using a water absorption test and water contact angle in which water absorption of 1175% in 180 min and water contact angle of 77.59° indicating a hydrophilic nature whereas the thermal characteristics are evaluated using TGA and DSC studies which confirmed the thermal stability of 22.92% at 800°C.

Keywords: Ameliorated chitosan, Chitosan, Membrane, Thermal studies, Spectroscopic studies, Water barrier studies

Introduction

The pursuit of sustainable and efficient materials has generated considerable interest in membranes made from biopolymers, namely those derived from chitosan. Chitosan is an extensively explored membrane material that shows tremendous potential[1]. Chitosan can be extracted from several sources such as crab shells, shrimp shells or fungal chitin and the choice of source of chitosan might affect the characteristics of the material[2,3]. Chitosan exhibits numerous distinctive characteristics due to its unique attributes that render its diverse applications such as membranes, hydrogels, beads, nanoparticles, sponges, interpenetrating and semi-penetrating networks which have numerous usages in industries such as wastewater treatment[2,4–6], drug delivery[7], wound healing[8], antimicrobial materials[9], food packaging[10], textiles[11], coatings[12], and energy storage materials[13]. The chitosan based materials are synthesized using different techniques such as template assisted synthesis[14], solution mixing or blending[15] , melt mixing[16], spray drying[17], in-situ synthesis[18], sol gel method[19], emulsion method[7], layer by layer assembly[20], electrospinning[21], co-precipitation[22], hydrothermal synthesis[23] and green synthesis [24].

The recent developments in membrane technology have concentrated on enhancing the effectiveness of chitosan membranes using several approaches. These methods involve integrating chitosan with different materials such as bio-active molecules, polymers, inorganic materials, metal ions and nanoparticles to improve its thermal, wettability, permeability and spectroscopic characteristics. These technological advances are designed to address the inherent limits of chitosan membranes such as modest thermal characteristics and vulnerability to degradation under specific conditions.

The water absorption behaviour of the polymer is influenced by different factors such as charge density, chemical composition, level of cross-linking, microstructure (porosity) of the polymer, the interaction between the polymer and water and environmental circumstances in which the polymer is placed [25]. Water absorption is a dynamic phenomenon that involves the simultaneous occurrence of mass movement and mechanical deformation. This phenomenon refers to the gradual change from a glassy or partial viscoelastic state to a viscoelastic (rubbery state)[26]. Diffusion refers to the movement of water molecules into the vacant areas between the polymeric chains. The diffusion of solvent molecules occurs at a slower pace compared to the relaxation of polymeric chains. As a result, the diffusion of solvent molecules regulates the swelling process, which

follows Fickian transport[27]. The network parameters such as mesh size, significantly influence the swelling behaviour of the membrane. The investigation on the graphene oxide and chitosan based mixed matrix membrane was developed in which it was observed that the water flux indicated an initial increase followed by a decrease as the concentration of graphene oxide was varied. The maximum flux was obtained for the 1 wt% which was attributed to the influence of the free volume of the membrane and hydrophilicity of the membrane[28]. The thermal and water barrier characteristics were investigated for the cellulose nanocrystals incorporated into the chitosan membrane through mechanical mixing and solution casting methods[29]. The swelling percentage indicated that it enhanced with time whereas the decreased as the concentration of cellulose nanocrystals content i.e., the pristine chitosan and 5 wt% composite showed a percentage of 1025.8% and 535.3%, respectively[29]. Another aspect of the water barrier was investigated using contact angle studies and the pristine membrane showed a contact angle of 67.9° whereas the contact angle was enhanced as the concentration of cellulose nanocrystals enhanced due to which at 5 wt% indicated a contact angle of 90.03° indicated a hydrophobic nature of the membrane[29]. With the increase in the cellulose nanocrystal content, there was a reduction in the carbon residue and an enhancement in the rigidity, crystallinity and heat resistance of the composite membranes[29]. The chitosan and TiO_2 based membranes were developed using simple casting in which it was observed that the higher concentration of TiO_2 indicated a lower water retention capacity whereas the composite membrane exhibited a lower mass loss in comparison to the pristine chitosan membrane[30]. The spectroscopic studies help to determine the chemical analysis, polymer composition, identification of functional groups, structural analysis, interaction studies, degradation studies and quality control[31].

The objective of the present study is to develop a chitosan membrane which was further characterized to study different characteristics such as spectroscopic characteristics, water barrier characteristics and thermal characteristics. The spectroscopic characteristics were evaluated using FT-IR and UV-visible-NIR absorption spectroscopy whereas the thermal characteristics were evaluated using TGA and DSC studies. The water barrier characteristics of the membrane were observed using the water absorption test and water contact angle.

Experimental Section

Materials

The following chemicals were utilized without additional purification: chitosan (analytical grade) from Hi-media, Mumbai, India. SD Fine Chemicals, Mumbai provided acetic acid and acrylic acid. Thiourea and potassium sulphate were provided by Merck and Loba Chemie. Millipore water was utilized for the formation of solutions and other polymeric processes. All chemicals were used without further purification.

Methods

Chitosan solution was prepared by dissolving 0.5 g chitosan flakes in 20 mL of 3% acetic acid solution which was kept overnight at room temperature. The viscous solution obtained was used for the synthesis of the ACM. A requisite amount of acrylamide (5 mol/L) was added dropwise to the filtered, homogenized, viscous chitosan solution under continuous stirring. The mixture was stirred for 10-20 min at room temperature. Subsequently, an appropriate amount of potassium persulfate was added to the homogeneous mixture to initiate the reaction with continuous stirring for another 20 min. Thiourea, serving as the crosslinker, was then added dropwise to the milky white solution. The mixture was maintained at 120°C for 60 min[4, 6]. The resulting gel was washed with Millipore water to remove any homopolymer and ACM was dried in an oven at 60°C until constant weight was achieved.

Optimization of different synthesis parameters

The synthesis of the ACM was carried out by optimizing different parameters such as the effect of the amount of solvent, the amount of monomer and the amount of initiator in terms of percentage grafting (P_g) which is also depicted using Fig. 1.

Effect of amount of solvent

The impact of the amount of solvent on the P_g was stidied by altering the volume of a 3% acetic acid solution, ranging from 5 to 25 mL. During the study, the amount of chitosan (0.5 g), amount of monomer (10 mL), amount of initiator (5 mL) and cross-linker (0.0025 mol/L) stayed the same. There was an increase in the P_g upto 15 mL i.e., 300% but on increasing the amount further there was a decrease in the P_g. It might be attributed to the polymerization reaction taking place with the help of OH• free radicals, the formation of $SO_4^{-\bullet}$ and the movement of

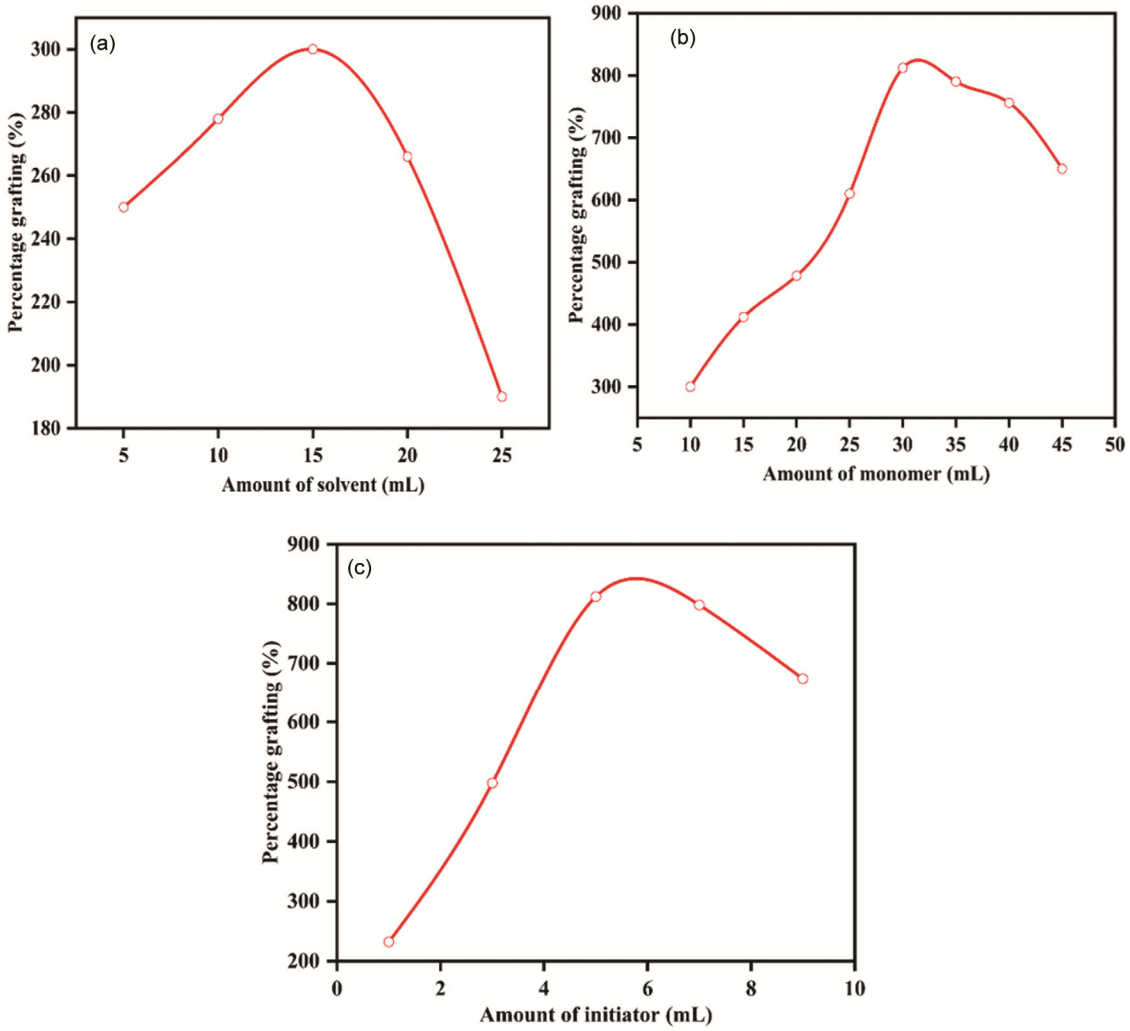

Fig. 1 — Effect on P_g w.r.t. amount of (a) initiator concentration, (b) monomer concentration and (c) solvent

ions towards the acrylic acid and backbone parts[4, 32, 33]. This process generates additional active sites on both vinyl monomer molecules and chitosan, assisted by the solvent volume. So, it made it easier for active poly(acrylic acid) chains to move to the active parts of the chitosan backbone, which resulted in a great rise in P_g.

Effect of amount of monomer

The impact of tailoring the amount of monomer on P_g was studied by varying the amount of monomer (5 mol/L) for a range of 10 to 45 mL at predefined parameters such as the amount of chitosan (0.5 g), amount of initiator concentration (5 mL), crosslinker (0.0025 mol/L) and amount of solvent (15 mL). It was observed that there was an increase in the P_g from 300 to 812% for the increase in the amount of monomer from 10 to 30 mol/L but on increasing the monomer amount further there was a decrease in the P_g which might be due to the enhanced inter and intra molecular self-crosslinking through secondary binding forces with diminished porous gel structure which developed the accumulation into the polymer matrix[4, 34].

Effect of amount of initiator

The effect of the amount of the initiator (0.025 mol/L) w.r.t. P_g at predefined parameters such as the amount of chitosan (0.5 g), crosslinker (0.0025 mol/L), amount of solvent (15 mL) and amount of monomer (30 mL) was studied. It was observed that there was an increase in the P_g from 232 to 812% for the amount of initiator of 1 to 5 mL. On increasing the amount further, it was observed that there was a decrease in the P_g. The initiator's primary function is to trigger the polymerization reaction

by generating $SO_4^{-\bullet}$ in the reaction medium. These species lead to the formation of numerous active sites on both chitosan backbone and monomer molecules. This ultimately leads to a higher degree of grafting of grafting of living polyvinyl chains onto chitosan, thereby achieving a high P_g value[4,6]. Even so, when the amount of initiators went up, homopolymerization rather than graft copolymerization became more common which was due to the active polyacrylic acid chains being made in the reaction medium.

Characterization techniques

Thermal gravimetric analysis was carried out using the Shimadzu DTG 60 TGA/DTG model. Differential scanning calorimetry (DSC) analysis was carried out using Waters TA instruments Q200 modulated DSC. Absorption spectroscopy was carried out using Agilent Cary 5000 UV-visible-NIR spectrophotometer. Fourier transform infrared spectroscopy (FTIR) was carried out using Thermo Fischer Scientific Nicolet iS50 FTIR tri-detector. FESEM micrographs were carried out using Zeiss Gemini SEM 500. The water contact angle of the membrane was obtained using Kruss DSA100. The water absorption of the membrane was studied over a period of time in which the initially dry weight of the membrane was obtained and after that, the weight submerged membrane was obtained at different intervals. The water absorption of the ACM was calculated using the formula given below[35–37].

$$Percentage\ water\ absorption = \frac{W_f - W_i}{W_i} * 100 \quad \ldots(2)$$

Results and Discussion

Spectroscopic studies

Fig. 2 shows the FTIR spectra of the chitosan and ACM in which it was observed that a prominent absorption peak at 3394 cm^{-1}, can be attributed to symmetrical stretching vibration of the -OH group. The distinctive absorption peaks of 1636 and 1551 cm^{-1}, are a result of the stretching vibration of the amino group[4,6]. A peak of 2846 cm^{-1}, corresponding to the symmetric $-CH_2$ stretching vibration of the pyranose ring, is found. The small peak observed at around 894 cm^{-1} corresponds to the oscillation of the saccharide arrangement in chitosan. In the case of ACM, a change in the absorption band occurs at 3318 cm^{-1}, which corresponds to the -OH group. It could be attributed to the heightened magnitude of this peak in the membrane to the polymerization of acrylic acid chains onto chitosan [6]. The distinct peak at 1067 cm^{-1} was seen, indicating the stretching of the C=S bond in the membrane. The peaks at 685 and 600 cm^{-1} are indicative of the bending vibration of the N-H and CH_2 rocking, respectively.

The UV-visible absorption spectra for the chitosan and ACM show absorption bands at 285 and 293 nm respectively, as shown in Fig. 3. It might be attributed to the $n \rightarrow \pi^*$ transition which involves the amine groups[38]. The peak at 285 nm and 293 nm peak are highlighted with the dashed line in Fig. 3.

Additionally, Fig. 4 illustrates the NIR absorption spectra of the chitosan and ACM. It was observed that the ACM showed major peaks at 1482 and 1969 nm whereas the chitosan showed peaks at 1532 nm, 1936 nm and 2025 nm. The intense peaks observed at 1482 nm, 1936 nm and 2025 nm might be attributed to the stretching and deformation of the O-H group whereas the absorption band observed at 1969 nm in ACM might be attributed to the hydrogen bonding and deacetylation of chitosan[39,40].

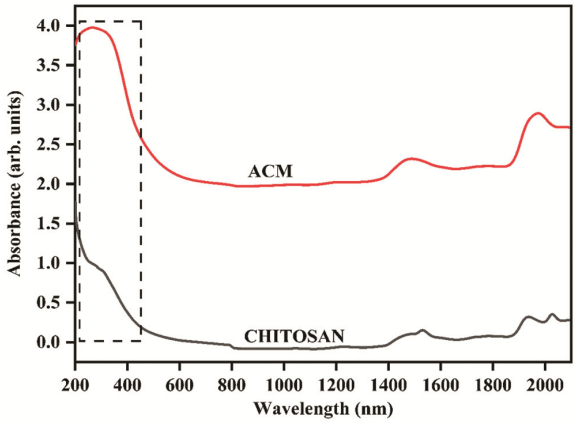

Fig. 2 — FTIR spectra of chitosan and ACM

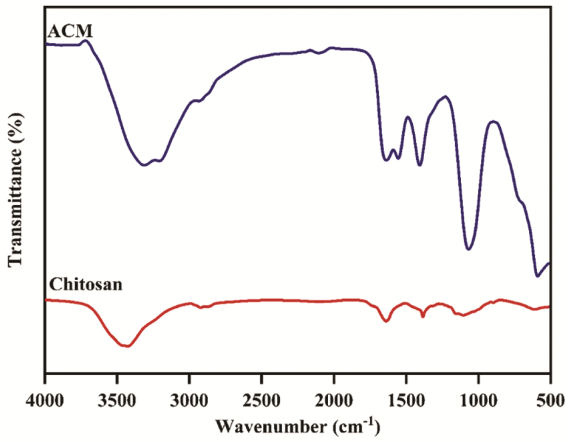

Fig. 3 — Absorption spectra of chitosan and ACM

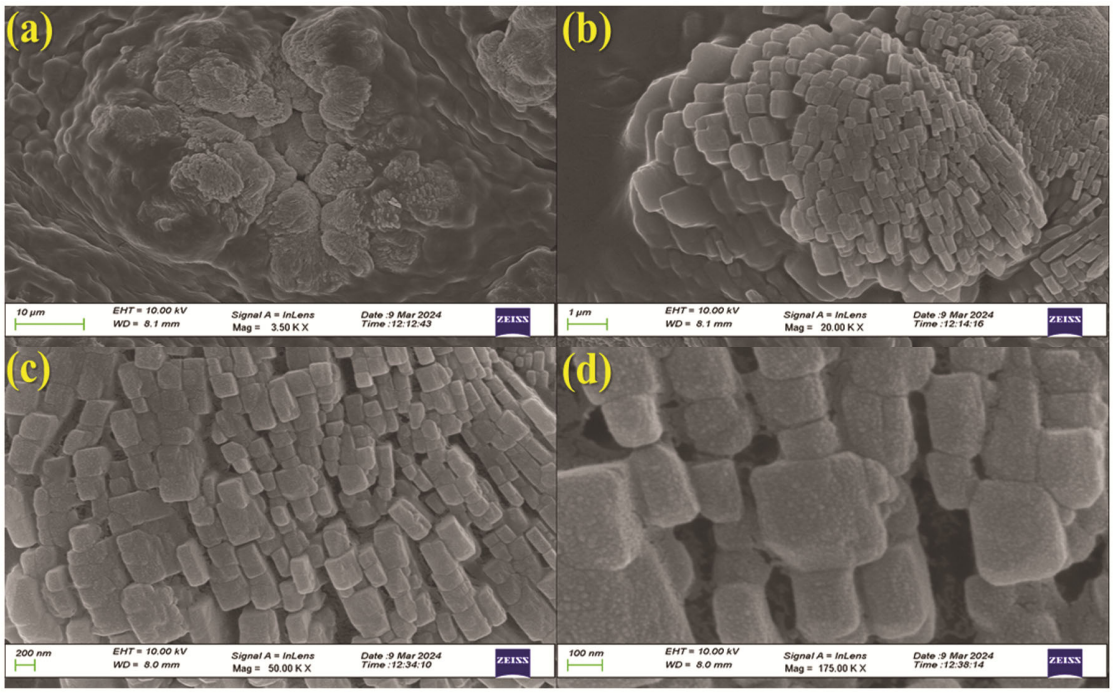

Fig. 5 — FESEM micrographs of ACM

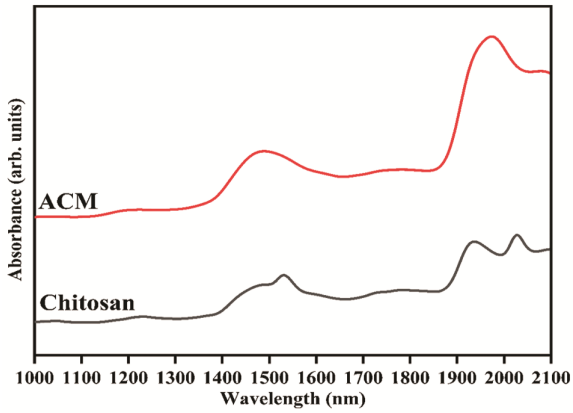

Fig. 4 — NIR absorption spectra of the chitosan and ACM

Morphology

FESEM micrographs of ACM are depicted in Fig. 5. It can be observed that the flower-like structures. When the micrographs were obtained at higher magnifications, the flower structure indicated a rod-like structure which might be attributed to the polymerization and grafting process which is also confirmed using FTIR spectra. Additionally, the presence of rod-like structures showed a specific arrangement of chitosan molecules in the microstructure which could be attributed to the obstruction of certain segments of chitosan during the synthesis process[41]. Interestingly, these rod structures are also capable of developing interconnected networks that generate multiple empty spaces and pathways, which results in increased porosity[42]. The gaps between the rods create more void space within the membrane, which encourages fluid or gas passage through the material which is depicted in the FESEM micrographs and also confirmed using the water absorption studies.

Thermal studies

The thermal studies for ACM were evaluated using thermogravimetric analysis and differential scanning calorimetry. The thermal characteristics of the membrane were studied using TGA which is depicted using Fig. 6. It was observed that the 20% and 50% thermal degradation of the membrane was observed at 230.66 and 302.10°C, respectively. Additionally, thermal stability was observed at 22.92% at 800°C. The TGA curve was used to plot the derivative curve which was used to calculate the ˚inflection point, T_{d1} (first peak of DTG) and the T_{d2} (second peak of DTG) which was found to be 234.54, 128.32°C and 255.40°C, respectively. When assessing the initial phase of deterioration, which involves the loss, the DTG curves show that their forms are dissimilar. Polysaccharides often exhibit a high affinity for water, making them easily hydrated and leading to the formation of macromolecules with rather disorganized structures. The hydration characteristics of these polysaccharides are dependent on their primary and

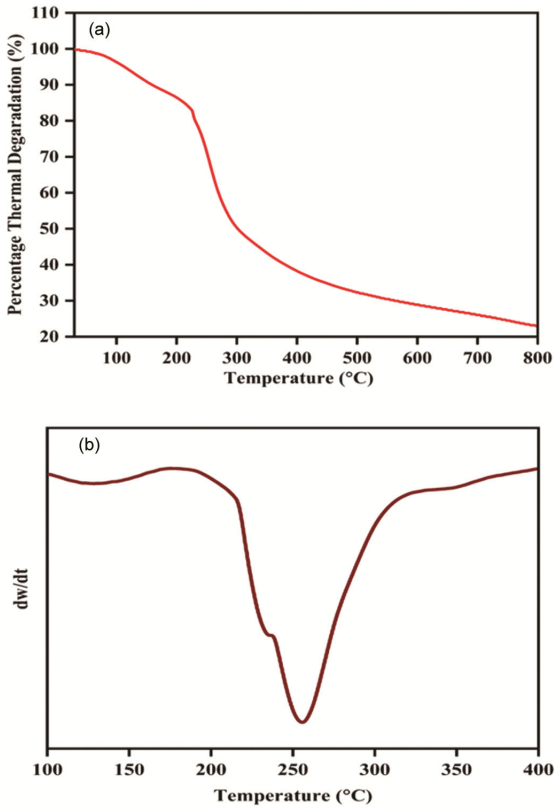

Fig. 6 — (a) TGA and (b) DTG curves of ACM

Table 1 — DSC data for the curve

S. No	Peak Temp. (°C)	Heat flow (mW)	Latent heat capacity (J g^{-1})	Peak type
1	100.32	-5.067	-120.5	Endothermic
2	199.26	-0.3629	-34.20	
3	227.39	-0.1034	-4.456	Exothermic
4	270.28	-0.1305	-11.95	

supramolecular structures. The thermal stability of 22.92% was observed at 800°C for the ACM. The literature indicated that for chitosan in the first phase, there was a reduction of 6.7% in the weight of the chitosan at 104°C due to the evaporation of both free and bound water molecules as well as other volatile chemicals[6]. The chemical bonds of the chitosan were disrupted and displayed a weight reduction of 38% at a temperature range of 225-325.5°C in the second stage of the thermal decomposition[6]. Interestingly, the final stages of decomposition showed a progressive reduction in the weight when the temperature of 631.6°C was attained due to the breakdown of the polysaccharide structure [6].

Additionally, the thermal assessment using DSC analysis as shown in Table 1 and Fig. 7 reveals the presence of endothermic and exothermic peaks for the

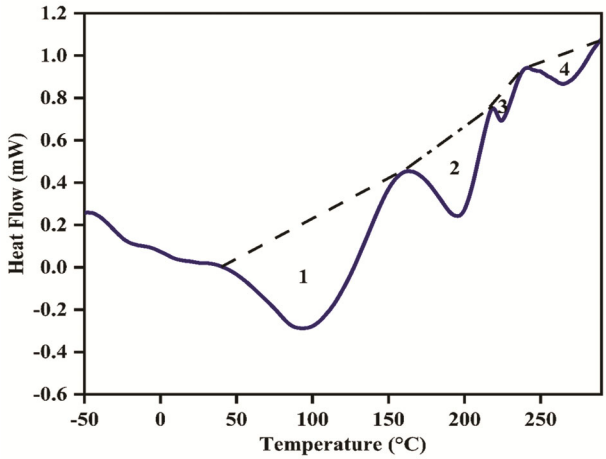

Fig. 7 — DSC curve of the ACM

range of 40-160°C and 210-280°C, respectively. The evaporation of water in the samples, occurring across a broad temperature range, causes this endotherm[43]. The endothermic peak suggest a larger water content in the sample which might be due to the introduction of additional hydrophilic sites into the membrane and which also corresponds to the water absorption test and water contact angle results. This is specifically due to the presence of polar functional groups like thiocarbonyl and amino groups which are capable of developing hydrogen bonds with the water molecules[44]. The literature showed that the glass transition temperature for chitosan at 203°C but for the case of ACM there is a shift towards the higher temperature which indicates better thermal characteristics and stability[45]. Additionally, it has been observed from Fig. 7 that as the temperature is being increased, there is a reduction in the amount of energy as the material shifts from endotherm to exotherm region which might be due to thermal decomposition of the ACM [46].

Water barrier studies

The water barrier studies were carried out using water absorption studies which were further studied with the help of a water absorption test and the wettability of the ACM. The water absorption pattern and water contact angle of ACM are depicted using Fig. 8 which depicts a water contact angle of 77.59° and the hydrophilic nature of the membrane. The enhanced water absorption can be attributed to the hydrophilicity of the ACM and the development of rod like structures that are capable of developing interconnected networks that generate multiple empty spaces and pathways, which resulted in enhanced porosity and is also confirmed using FESEM

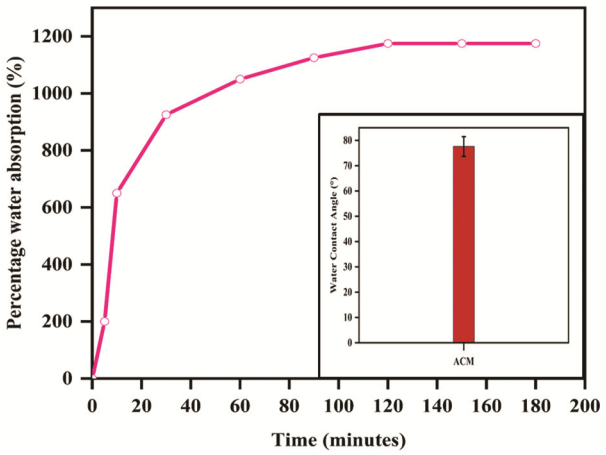

Fig. 8 — Water absorption behaviour and water contact angle of the ACM

micrographs[42,47]. The chitosan crosslinked with glutaraldehyde indicated helped in developing the hydrophobic structures which helped in confirming the effect of the degree of glutaraldehyde incorporation[48].

Conclusion

The ACM showed effective thermal, spectroscopic and water barrier characteristics. The development of the membrane was confirmed using the FTIR and UV-visible-NIR spectroscopy studies. Thermal studies such as TGA confirm the thermal stability of 22.92% at 800°C for the ACM whereas the endotherm and exotherm for the ACM were confirmed from the DSC studies. The water barrier studies depicted a water absorption of 1175% at 180 min and depicted a water contact angle of 77.59° indicating a hydrophilic nature of the membrane.

Acknowledgment

The authors would like to thank the University Science Instrumentation Centre (USIC), University of Delhi for providing the necessary support for different characterization techniques.

References

1 Ge J, Cui Y, Yan Y & Jiang W, The effect of structure on pervaporation of chitosan membrane, *J Memb Sci*, 165 (2000) 75.

2 Bhullar N K, Sachdev D & Kumari K, Applications of chitosan based materials in wastewater systems, In: Futuristic Trends in Chemical, *Mater Sci Nano Technol*, (2024) 74.Please provide volume number

3 Meena H M, Kukreti S & Jassal P S, Adsorption and estimation of As (III) from wastewater using cross linked Chitosan-STPP nanoparticles with voltammetric analysis computrace, isotherms, and kinetic study, *Results Eng*, 23 (2024) 102467.

4 Bhullar N, Kumari K & Sud D, A biopolymer-based composite hydrogel for rhodamine 6G dye removal: Its synthesis, adsorption isotherms and kinetics, *Iranian Polym J*, 27 (2018) 527.

5 Bhullar N, Rani S, Kumari K & Sud D, Amphiphilic chitosan/acrylic acid/thiourea based semi-interpenetrating hydrogel: Solvothermal synthesis and evaluation for controlled release of organophosphate pesticide, triazophos, *J Appl Polym Sci*, 138 (2021) 50595.

6 Bhullar N K, Kumari K & Sud D, Semi-interpenetrating networks of biopolymer chitosan/acrylic acid and thiourea hydrogels: Synthesis, characterization and their potential for removal of cadmium, *Iranian Polym J*, 28 (2019) 225.

7 Khan T A, Azad A K, Fuloria S, Nawaz A, Subramaniyan V, Akhlaq M, Safdar M, Sathasivam K V, Sekar M, Porwal O, Meenakshi D U, Malviya R, Miret M M, Mendiratta A & Fuloria N K, Chitosan-coated 5-fluorouracil incorporated emulsions as transdermal drug delivery matrices, *Polymers*, 13 (2021) 3345.

8 Najafabadi S A A, Mohammadi A & Kharazi A Z, Polyurethane nanocomposite impregnated with chitosan-modified graphene oxide as a potential antibacterial wound dressing, *Mater Sci Eng: C*, 115 (2020) 110899.

9 Huq M A, Ashrafudoulla M, Parvez M A K, Balusamy S R, Rahman M M, Kim J H & Akter S, Chitosan-coated polymeric silver and gold nanoparticles: Biosynthesis, characterization and potential antibacterial applications: A Review, *Polymers*, 14 (2022) 5302.

10 Al-Naamani L, Dobretsov S & Dutta J, Chitosan-zinc oxide nanoparticle composite coating for active food packaging applications, *Innov Food Sci Emerg Technol*, 38 (2016) 231.

11 Zhou C E, Kan C W, Sun C, Du J & Xu C, A review of chitosan textile applications, *AATCC J Res*, 6 (2022) 8.

12 Andrade-del-Olmo J, Pérez-Álvarez L, Sáez-Martínez V, Benito-Cid S, Ruiz-Rubio L, Pérez-González R, Vilas-Vilela J L & Alonso J M, Multifunctional antibacterial chitosan-based hydrogel coatings on Ti_6Al_4V biomaterial for biomedical implant applications, *Int J Biol Macromol*, 231 (2023) 123328.

13 Siddiqui M T H, Baloch H A, Nizamuddin S, Mubarak N M, Hossain N, Zavabeti A, Mazari S A, Griffin G J & Srinivasan M, Synthesis and optimization of chitosan supported magnetic carbon bio-nanocomposites and bio-oil production by solvothermal carbonization co-precipitation for advanced energy applications, *Renew Energy*, 178 (2021) 587.

14 Kaur A, Bajaj B, Kaushik A, Saini A & Sud D, A review on template assisted synthesis of multi-functional metal oxide nanostructures: Status and prospects, *Mater Sci Eng: B*, 286 (2022) 116005.

15 Giannakas A, Patsaoura A, Barkoula N M & Ladavos A, A novel solution blending method for using olive oil and corn oil as plasticizers in chitosan based organoclay nanocomposites, *Carbohydr Polym*, 157 (2017) 550.

16 Correlo V M, Boesel L F, Bhattacharya M, Mano J F, Neves N M & Reis R L, Properties of melt processed chitosan and aliphatic polyester blends, *Mater Sci Eng: A*, 403 (2005) 57.

17 Ngan L T K, Wang S L, Hiep I M, Luong P M, Vui N T, Crossed T M, Signinh D & Dzung N A, Preparation of chitosan nanoparticles by spray drying, and their antibacterial activity, *Res Chem Intermediate*, 40 (2014) 2165.

18 Li M, Wang Y, Liu Q, Li Q, Cheng Y, Zheng Y, Xi T & Wei S, In situ synthesis and biocompatibility of nano

hydroxyapatite on pristine and chitosan functionalized graphene oxide, *J Mater Chem B*, 1 (2012) 475.
19 Budnyak T M, Pylypchuk I V, Tertykh V A, Yanovska E S & Kolodynska D, Synthesis and adsorption properties of chitosan-silica nanocomposite prepared by sol-gel method, *Nanoscale Res Lett*, 10 (2015) 1.
20 Zhou J, Romero G, Rojas E, Ma L, Moya S & Gao C, Layer by layer chitosan/alginate coatings on poly(lactide-co-glycolide) nanoparticles for antifouling protection and folic acid binding to achieve selective cell targeting, *J Colloid Interface Sci*, 345 (2010) 241.
21 Augustine R, Rehman S R U, Ahmed R, Zahid A A, Sharifi M, Falahati M & Hasan A, Electrospun chitosan membranes containing bioactive and therapeutic agents for enhanced wound healing, *Int J Biol Macromol*, 156 (2020) 153.
22 Pu S, Hou Y, Yan C, Ma H, Huang H, Shi Q, Mandal S, Diao Z & Chu W, In situ coprecipitation formed highly water-dispersible magnetic chitosan nanopowder for removal of heavy metals and its adsorption mechanism, *ACS Sustain Chem Eng*, 6 (2018) 16754.
23 Yang Y, Cui J, Zheng M, Hu C, Tan S, Xiao Y, Yang Q & Liu Y, One-step synthesis of amino-functionalized fluorescent carbon nanoparticles by hydrothermal carbonization of chitosan, *Chem Commun*, 48 (2011) 380.
24 Kazemi M S & Sobhani A, $CuMn_2O_4$/chitosan micro/nanocomposite: Green synthesis, methylene blue removal, and study of kinetic adsorption, adsorption isotherm experiments, mechanism and adsorbent capacity, *Arab J Chem*, 16 (2023) 104754.
25 Ceylan D, Ozmen M M & Okay O, Swelling-deswelling kinetics of ionic poly(acrylamide) hydrogels and cryogels, *J Appl Polym Sci*, 99 (2006) 319.
26 Ganji F, Vasheghani-Farahani S & Vasheghani-Farahani E, Theoretical description of hydrogel swelling: A review, 19 (2010) 375.
27 Bajpai A K, Shukla S K, Bhanu S & Kankane S, Responsive polymers in controlled drug delivery, *Prog Polym Sci*, 33 (2008) 1088.
28 Qian X, Li N, Wang Q & Ji S, Chitosan/graphene oxide mixed matrix membrane with enhanced water permeability for high-salinity water desalination by pervaporation, *Desalination*, 438 (2018) 83.
29 Mao H, Wei C, Gong Y, Wang S & Ding W, Mechanical and water-resistant properties of eco-friendly chitosan membrane reinforced with cellulose nanocrystals, *Polymers*, 11 (2019) 166.
30 Spoială A, Ilie C I, Dolete G, Croitoru A M, Surdu V A, Trușcă R D, Motelica L, Oprea O C, Ficai D, Ficai A, Andronescu E & Dițu L M, Preparation and characterization of chitosan/TiO_2 composite membranes as adsorbent materials for water purification, *Membranes*, 12 (2022) 804.
31 Sachdev D, Jha P K, Rani R, Verma G, Kaur N & Sahu O, Structural and optical investigation of highly fluorescent tartaric acid derived from the tamarind pulp, *Mater Chem Phys*, 296 (2023) 127294.
32 Kaith B S, Jindal R & Maiti M, Induction of chemical and moisture resistance in Saccharum spontaneum L fiber through graft copolymerization with methyl methacrylate and study of morphological changes, *J Appl Polym Sci*, 113 (2009) 1781.
33 Kaith B S, Jindal R, Jana A K & Maiti M, Characterization and evaluation of methyl methacrylate-acetylated Saccharum spontaneum L. graft copolymers prepared under microwave, *Carbohydr Polym*, 78 (2009) 987.
34 Jindal R, Kaith B S & Mittal H, Rapid synthesis of acrylamide onto xanthan gum based hydrogels under microwave radiations for enhanced thermal and chemical modifications, *Polym Renew Resour*, 2 (2011) 105.
35 Li Y, Ma Z, Yang X, Gao Y, Ren Y, Li Q, Qu Y, Chen G & Zeng R, Investigation into the physical properties, antioxidant and antibacterial activity of Bletilla striata polysaccharide/chitosan membranes, *Int J Biol Macromol*, 182 (2021) 311.
36 Sachdev D, Shah K, Sharma D, Verma G, Kaur N & Sahu O, Adsorptive removal of methylene blue dye by extracted banana stem fibers, *Mater Today Proc*, 68 (2022) 728.
37 Sachdev D, Shrivastava H, Kajal, Sharma S, Sanjeev, Srivastava S, Tadepalli S, Bhullar N K & Sahu O P, Potential for hydrothermally separated groundnut shell fibers for removal of methylene blue dye, *Mater Today Proc*, 48 (2022) 1559.
38 D.A. Skoog, F.J. Holler & S.R. Crouch, *Principles of Instrumental Analysis*, 7th Edition,Cengage Learning, (2017).
39 Cazón P, Cazón D, Vázquez M & Guerra-Rodriguez E, Rapid authentication and composition determination of cellulose films by UV-VIS-NIR spectroscopy, *Food Packag Shelf Life*, 31 (2022) 100791.
40 Venkatesh K, Nalluri V R, Barla V S, Gandhi R R & Kumar R, A practical evaluation of qualitative and quantitative chemometric models for real-time monitoring of moisture content in a fluidised bed dryer using near infrared technology, *J Near Infrared Spectrosc*, 22 (2014) 221.
41 Sarma G K, Sharma R, Saikia R, Borgohain X, Iraqui S, Bhattacharyya K G & Rashid M H, Facile synthesis of chitosan-modified ZnO/$ZnFe_2O_4$ nanocomposites for effective remediation of groundwater fluoride, *Environ Sci Pollut Res*, 27 (2020) 30067.
42 Esparza-Flores E E, Siquiera L B, Cardoso F D, Costa T H, Benvenutti E V, Medina-Ramírez I E, Perullini M, Santagapita P R, Rodrigues R C & Hertz P F, Chitosan with modified porosity and crosslinked with genipin: A dynamic system structurally characterized, *Food Hydrocoll*, 144 (2023) 109034.
43 Rueda D R, Secall T & Bayer R K, Differences in the interaction of water with starch and chitosan films as revealed by infrared spectroscopy and differential scanning calorimetry, *Carbohydr Polym*, 40 (1999) 49.
44 Yong T, Wu F, Xiao H & Wan B, Silica modified with a thiourea derivative as a new stationary phase for hydrophilic interaction liquid chromatography, *J Sep Sci*, 38 (2015) 3852.
45 Sakurai K, Maegawa T & Takahashi T, Glass transition temperature of chitosan and miscibility of chitosan/poly(N-vinyl pyrrolidone) blends, *Polymer*, 41 (2000) 7051.
46 Müller A J & Michell R M, Differential scanning calorimetry of polymers, *Polymer Morphology: Principles, Characterization and Process*, (2016) 72–99.
47 Erceg T, Dapčević-Hadnađev T, Hadnađev M & Ristić I, Swelling kinetics and rheological behaviour of microwave synthesized poly(acrylamide-co-acrylic acid) hydrogels, *Colloid Polym Sci*, 299 (2021) 11.
48 Beppu M M, Vieira R S, Aimoli C G & Santana C C, Crosslinking of chitosan membranes using glutaraldehyde: Effect on ion permeability and water absorption, *J Memb Sci*, 301 (2007) 126.